

# Distribution of the Cobalt-Containing Component in the Pore Space of HZSM-5 upon a Postsynthetic Modification of the Zeolite with Hydroxo Compounds of $\text{Co}^{2+}$

O. P. Krivoruchko, V. Yu. Gavrilov, I. Yu. Molina, and T. V. Larina

Boreskov Institute of Catalysis, Siberian Branch, Russian Academy of Sciences, Novosibirsk, 630090 Russia

e-mail: opkriv@catalysis.nsk.su, gavrilov@catalysis.nsk.su

Received October 3, 2006

**Abstract**—The distribution of the cobalt-containing modifying component in the pore space of zeolite HZSM-5 depending on the total cobalt content of the samples (0.5–5.0 wt %) was quantitatively studied for the first time. At cobalt concentrations to 3.0 wt %, the cobalt-containing modifying component mainly occurred as isolated  $\text{Co}_{\text{Oh}}^{2+}$  ions in the micropores (channels) of HZSM-5 at the ion-exchange positions of the zeolite and in one-dimensional  $\text{CoO}$  and  $\text{CoAl}_2\text{O}_4$  nanoclusters. A further increase in the cobalt concentration to 5.0 wt % resulted, in addition to the filling of micropores, in the partial filling of the mesopore space of the zeolite with a small amount of three-dimensional  $\text{CoO}$  and  $\text{CoAl}_2\text{O}_4$  nanoparticles. Using sorption data and electronic diffuse reflectance spectra, we were the first to find that the effective density of a cobalt-containing modifying component in the pore space of a zeolite matrix was lower than the density of a bulk  $\text{CoO}$  phase by a factor of 6.

**DOI:** 10.1134/S0023158408020171

## INTRODUCTION

Unusual adsorption and catalytic properties of high-silica zeolites modified with doubly charged cations, in particular,  $\text{Co}^{2+}$  ions, have attracted considerable attention in the last few years [1–6]. Thus, the adsorption of  $\text{H}_2$  on CoZSM-5 samples was detected [1]; hypothetically, this adsorption occurred at the  $\text{Co}^{2+}$  ions stabilized outside the tetrahedral positions of the zeolite framework. The CoZSM-5 catalysts exhibited high activity in the reactions of selective  $\text{NO}_x$  reduction [2], ethane ammoxidation to acetonitrile [3, 4], complete hydrocarbon oxidation [5, 6], etc. The activity and selectivity of these catalysts was related to not only the state of  $\text{Co}^{2+}$  ions but also the character of their localization in the pore space of high-silica zeolites.

The  $\text{Co}^{2+}$  ions can be introduced into the framework of only some types of zeolites and only at the stage of zeolite synthesis from mixed gels. Thus, CoAPO-5 zeolites, whose framework contained  $\text{Co}^{2+}$  ions in a tetrahedral ( $\text{Co}_{\text{Td}}^{2+}$ ) oxygen coordination, were synthesized from gels containing  $\text{Co}^{2+}$ ,  $\text{Al}^{3+}$ , and  $\text{PO}_4^{3-}$  [7]. The isomorphous replacement of  $\text{Al}^{3+}$  ions at tetrahedral positions ( $\text{Al}_{\text{Td}}^{3+}$ ) by  $\text{Co}^{2+}$  ions in the framework of the formed HZSM-5 zeolite cannot be performed using so-called postsynthetic modification.

The postsynthetic modification is most frequently performed by wet or solid-phase ion exchange between  $\text{M}^{2+}$  salts and various zeolites [8]. In accordance with a

currently widespread opinion,  $\text{M}^{2+}$  ions are localized in the channels of zeolite HZSM-5 at the following three types of charge-exchange sites [9, 10]:

(1)  $\text{M}^{2+}$  is coordinated to two of four oxygen atoms from the environment of isolated aluminum atoms and contains one OH group in the coordination sphere (these sites are designated as  $\text{Z}^-\text{[MeOH]}^+$ );

(2)  $\text{M}^{2+}$  is coordinated to oxygen of a pair of aluminum atoms contained in six-membered rings (designated as  $\text{Z}^-\text{Me}^{2+}\text{Z}^-$ );

(3)  $\text{M}^{2+}$  is coordinated to oxygen of a pair of aluminum atoms separated by a  $\text{Si}_{\text{Td}}^{4+}$  atom as  $[\text{Me}-\text{O}-\text{M}]^{2+}$  dimers (designated as  $\text{Z}^-\text{[MOM]}^2\text{Z}^-$ ).

Two main assumptions form the basis of these concepts. First, the localization of  $\text{M}^{2+}$  ions occurs only at oxygen atoms bound to  $\text{Al}_{\text{Td}}^{3+}$  in zeolite HZSM-5 channel walls. Second, all of the aluminum contained in zeolite is framework aluminum. At the same time, the channels of zeolite HZSM-5 (particularly, with a Si/Al ratio of  $\leq 20$ ) almost always contain extraframework aluminum [11], the appearance of which can be a consequence of the incomplete interaction of components in the synthesis of zeolites or the subsequent thermal treatment of these zeolites. Before our previous study [12], the possible interaction of  $\text{M}^{2+}$  ions introduced into the channels of zeolite HZSM-5 with the extraframework aluminum had not been detected experimentally and this possibility had not even been discussed.

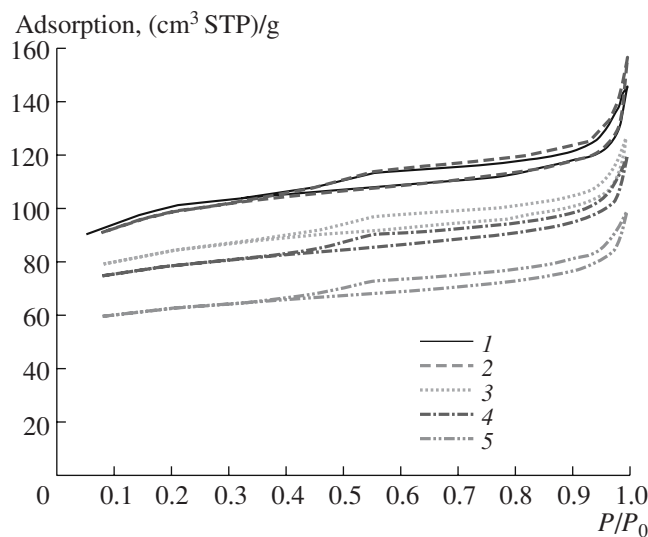


**Fig. 1.** Isotherms of nitrogen adsorption on (1) parent zeolite HZSM-5 and modified Co(*n*)ZSM-5 samples containing (2) 0.5, (3) 2.0, (4) 3.0, and (5) 5.0 wt % Co at 77 K.

Previously [12], we found that the introduction of doubly charged cations into high-silica zeolites followed by the hydrolytic polycondensation and the thermal treatment of samples provides an opportunity to stabilize M<sup>2+</sup> ions in zeolite channels in the following three forms: as isolated M<sub>OH</sub><sup>2+</sup> ions at ion-exchange positions; in a tetrahedral coordination, which is unusual for these systems, due to the interaction with extraframework Al<sup>3+</sup> with the formation of one-dimensional M<sup>2+</sup>Al<sub>2</sub>O<sub>4</sub> analogs; and as one-dimensional M<sup>2+</sup> oxide nanoclusters. At the same time, we did not study the distribution of a modifying component in the pore space of HZSM-5 crystals depending on the total cobalt content of the samples.

The aim of this work was to study the distribution and electronic state of a cobalt-containing component in the pore space of HZSM-5 upon the postsynthetic modification of the zeolite at 0.5–5.0 wt % cobalt concentrations in the samples.

## EXPERIMENTAL

A series of Co(*n*)ZSM-5 samples, where *n* is the cobalt content from 0.5 to 5.0 wt % of zeolite weight, were synthesized in this study. Commercial zeolite HZSM-5 with the ratio Si/Al = 17 and Fe<sup>3+</sup> and Na<sup>+</sup> impurity concentrations of 0.09 and 0.05 wt %, respectively, without a binding agent was used for the synthesis of Co<sup>2+</sup>ZSM-5; this zeolite was studied in detail previously [12]. Before the introduction of Co<sup>2+</sup> ions, the zeolite was calcined at 300°C to constant weight. Cobalt was introduced into zeolite channels by incipient wetness impregnation with aqueous solutions of CoCl<sub>2</sub> followed by the treatment of the samples with a

dilute solution of NH<sub>3</sub> at pH 9.0 and room temperature for 16 h. Next, the samples were filtered off, washed with distilled water, and kept in air to a dry state. At the final stage of the synthesis, the samples were calcined stepwise at 110, 250, 350, and 450°C in air for 6 h at each of the specified temperatures. Here, the results of a study of the samples calcined at a final temperature of 450°C are reported.

The pore structure of zeolite HZSM-5 and the samples modified with cobalt chloride was studied by the low-temperature (77 K) adsorption of N<sub>2</sub> using a Micromeritics Degasorb 2600 instrument. The samples were thermally pretreated in a vacuum at 450°C and a residual pressure of 10<sup>-3</sup> Torr for 5 h. The adsorption isotherms were treated using a comparative method [13] and the Barrett–Joyner–Halenda (BJH) method [14].

The diffuse reflectance electronic spectra were measured on a Shimadzu UV-2501 PC spectrophotometer equipped with an ISR-240 A diffuse reflectance accessory. The spectra were measured with reference to a BaSO<sub>4</sub> reflectance standard over the range 11000–53000 cm<sup>-1</sup>. The diffuse reflectance spectroscopy data were represented as the Kubelka–Munk function *F*(*R*).

The X-ray diffraction patterns of HZSM-5 and Co(*n*)ZSM-5 samples were measured on a Siemens D-500 diffractometer using CuK<sub>α</sub> radiation. A reflected-beam graphite monochromator was used to filter off CuK<sub>β</sub> radiation. The measurements were performed by scanning with a step of 0.05° and an accumulation time of 3 s in the range of angles 2θ = 5°–60°.

## RESULTS AND DISCUSSION

Figure 1 shows the isotherms of low-temperature nitrogen adsorption; these isotherms indicate that the test samples were characterized by developed micro- and mesoporosity. Table 1 summarizes the main structure parameters calculated from the sorption data by a comparative method. For a correct comparison, the parameters (*P*) in Table 1 are referred to a gram of zeolite in the catalyst in accordance with the relation *P*(1 + *X*), where *X* is the weight ratio between cobalt and zeolite, (g Co)/(g zeolite). As follows from Table 1, zeolite modification with Co<sup>2+</sup> compounds resulted in a noticeable change in the micropore component of the texture (a decrease in the micropore volume *V*<sub>μ</sub>), whereas the mesopore structure (probably, space between zeolite crystallites) changed to a much lesser degree (*V*<sub>cum</sub> and *S*<sub>in</sub>).

Figure 2 compares the isotherms of desorption for the parent zeolite HZSM-5 and the modified Co(*n*)ZSM-5 samples. It can be seen that, in the majority of cases, the comparative isotherm plots exhibited two linear portions I and II. In accordance with the pressure ranges of sorbate vapor, the former and latter portions correspond to sorption in the micropore and mesopore spaces of the zeolite, respectively. An analy-

**Table 1.** Texture parameters of parent zeolite HZSM-5 and modified Co(*n*)ZSM-5 samples

Cobalt concentration in HZSM-5, %	$V_\mu$ , $\text{cm}^3/\text{g}$	$S_\alpha$ , $\text{m}^2/\text{g}$	$V_{\text{pore}}$ , $\text{cm}^3/\text{g}$	$S_{\text{in}}$ , $\text{m}^2/\text{g}$	Slope*		$V_{\text{cum}}$ , $\text{cm}^3/\text{g}$	$V_{D < 5}$ , $\text{cm}^3/\text{g}$
					portion I	portion II		
0	0.122	77	0.153	32	1	1	0.098	0.046
0.5	0.111	95	0.151	36	1.12	1.10	0.111	0.055
2.0	0.098	79	0.135	28	0.90	0.88	0.096	0.046
3.0	0.097	64	0.128	27	0.76	0.89	0.094	0.040
5.0	0.079	53	0.103	26	0.61	0.81	0.080	0.034

Note:  $V_\mu$  is the micropore volume,  $S_\alpha$  is the mesopore surface area,  $V_{\text{pore}}$  is the total pore volume,  $S_{\text{in}}$  is the macropore surface area,  $V_{\text{cum}}$  is the cumulative mesopore volume calculated by the BJH method, and  $V_{D < 5}$  is the volume of mesopores with  $D < 5 \text{ nm}$ .

\* See the text for comments.

sis of the slopes of these portions (see Table 1) indicated that the slope of the former portion noticeably decreased in the course of modification (this corresponds to a relative decrease in the micropore volume of these samples), whereas the slope of the latter portion changed to a lesser extent to demonstrate the retention of the major portion of the pore space of mesopores. Note that, in a sample with a minimum concentration of the modifying component, the slopes of both of the portions were somewhat greater than unity; this suggests an increase in the micro- and mesopore volumes as compared with those of the parent zeolite. An analogous increase in the mesopore volume of this sample also follows from data on  $V_{\text{cum}}$  (Table 1). This fact remains to be explained.

The insert in Fig. 2 shows a correlation of the slope of portion I (relative decrease in the micropore volume) with the Co content of modified Co(*n*)ZSM-5 samples.

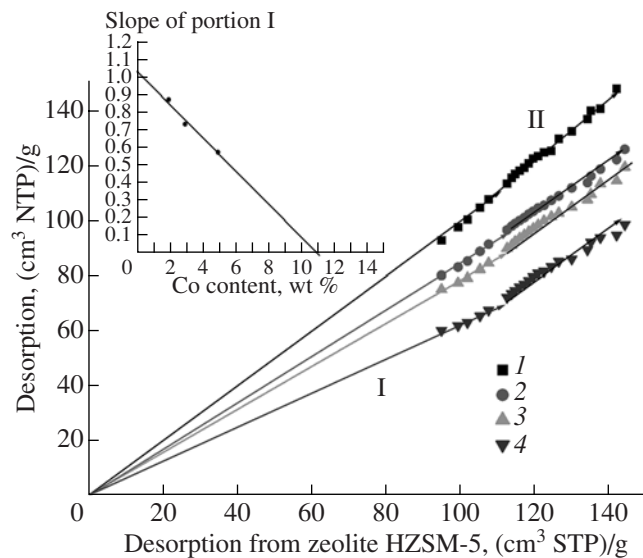
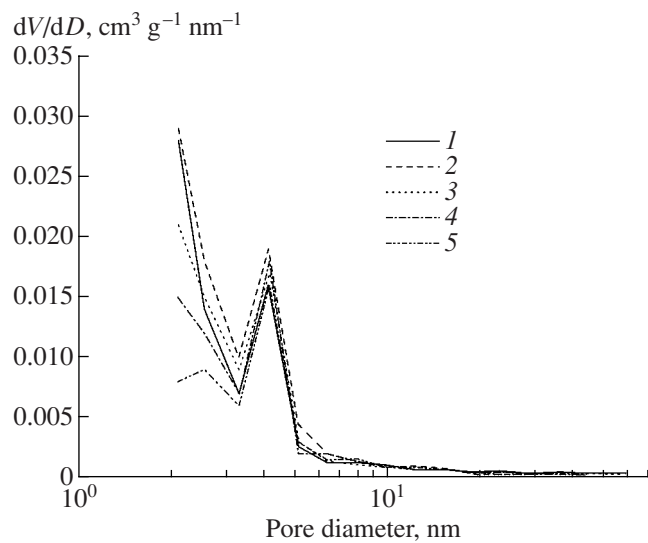


**Fig. 2.** Comparison between the isotherms of desorption from parent zeolite HZSM-5 and modified Co(*n*)ZSM-5 samples containing (1) 0.5, (2) 2.0, (3) 3.0, and (4) 5.0 wt % Co.

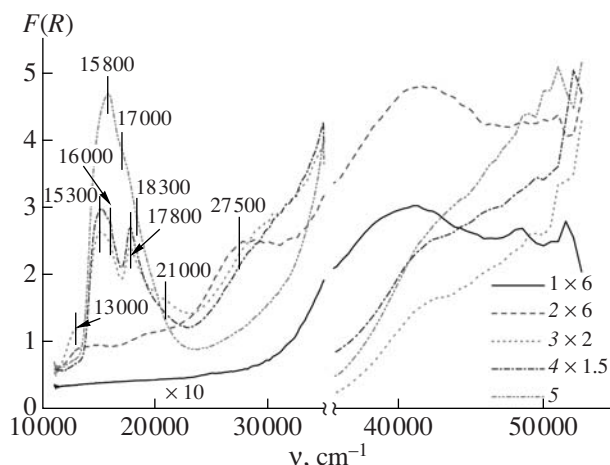
A stable linear correlation (except for the sample with a minimum cobalt content, which is not shown in the insert of Fig. 2) suggests an approximately constant effective density of the modifying component arranged in zeolite micropores.

Figure 3 shows differential mesopore-size distribution curves calculated by the BJH method. A comparison between the curves indicates that the volumes of the finest mesopores ( $D < 5 \text{ nm}$ ) decreased as the total amount of the modifying component was increased. In this case, the volume of fine mesopores in a sample with 0.5 wt % Co was higher than the corresponding volume in the parent zeolite (see  $V_{D < 5}$  in Table 1). At the same time, the pore space volume with  $D > 5 \text{ nm}$  remained almost unchanged.

An analysis of the above experimental data allowed us to conclude that, depending on the concentration of introduced cobalt, the modifying additive was localized



**Fig. 3.** Mesopore size distribution for (1) parent zeolite HZSM-5 and modified zeolite Co(*n*)ZSM-5 samples containing (2) 0.5, (3) 2.0, (4) 3.0, and (5) 5.0 wt % Co.



**Fig. 4.** Diffuse reflectance electronic spectra of (1) parent zeolite HZSM-5 and modified Co(*n*)ZSM-5 samples containing (2) 0.5, (3) 2.0, (4) 3.0, and (5) 5.0 wt % Co.

in both the micropore volume and the mesoporous portion of the zeolite structure, mainly, with the pore sizes  $D < 5$  nm. The quantitative relationship between the volumes of the modifying component arranged in zeolite micro- and mesopores will be analyzed below.

Let us consider the experimental data on the electronic state of the cobalt-containing modifying component in the pore space of Co(*n*)ZSM-5 samples.

The electronic states of cobalt ions in various coordination environments have been much studied [15]. Together with the results of the previous study [12] of zeolites CoZSM-5, these published data [12, 15] form a basis for the reliable interpretation of the diffuse reflectance electronic spectroscopy data given below.

At 0.5–3.0 wt % cobalt concentrations in the samples, the modifying component almost completely occurred in the micropores (channels) of zeolite HZSM-5 (see Table 1). Because the size of cylindrical channels in HZSM-5 crystals is  $\sim 0.55$  nm, it is reasonable to consider the modifying component in this region of Co(*n*)ZSM-5 sample compositions to be composed of one-dimensional nanoclusters. At a cobalt content of the samples higher than 3.0 wt %, a portion of this component is arranged in mesopores (see Table 1). In these samples, two- and three-dimensional nanoparticles of the cobalt-containing modifying components are formed along with one-dimensional nanoparticles.

Figure 4 shows the diffuse reflectance electronic spectra of zeolite HZSM-5 and the samples prepared by zeolite modification with cobalt cations with concentrations from 0.5 to 5.0 wt %. The parent zeolite (Fig. 4, curve 1) was characterized by the appearance of the fundamental absorption edge in the UV region at  $37500\text{ cm}^{-1}$  due to the occurrence of a band gap, which is typical of dielectric oxide structures, in the zeolite [16]. The absence of absorption bands due to the

absorption of zeolite as a whole from the visible region of the diffuse reflectance electronic spectra of parent HZSM-5 allowed us to unambiguously interpret absorption bands, which characterize the electronic state of cobalt in the modifying component of Co(*n*)ZSM-5 samples.

The diffuse reflectance electronic spectrum of a Co(0.5)ZSM-5 sample (Fig. 4, curve 2) exhibited an absorption band at  $27500\text{ cm}^{-1}$ , whose intensity decreased as the cobalt content of the modified sample was further increased. It is likely that this absorption band appeared due to the state of  $\text{Co}^{2+}$ , which is difficult to interpret unambiguously. Note that the diffuse reflectance electronic spectrum of the Co(0.5)ZSM-5 sample also exhibited two low-intensity broad absorption bands in the visible region at  $13000$ – $17000$  and  $17500$ – $20000\text{ cm}^{-1}$ . The broadening of these absorption bands allowed us to assume the occurrence of heterogeneously distributed  $\text{Co}^{2+}$  cations in both tetrahedral and octahedral ( $\text{Co}_{\text{Oh}}^{2+}$ ) oxygen coordinations in zeolite channels. It is likely that  $\text{Co}_{\text{Oh}}^{2+}$  cations were localized at ion-exchange positions in the zeolite channels. Taking into account that the intensity of absorption bands due to  $\text{Co}_{\text{Oh}}^{2+}$  ions was higher than that of absorption bands due to  $\text{Co}_{\text{Td}}^{2+}$  ions by two orders of magnitude, we can conclude that cobalt cations in the Co(0.5)ZSM-5 sample mainly occurred in the  $\text{Co}_{\text{Oh}}^{2+}$  state.

As the cobalt content was increased to 2.0 wt % or higher (Fig. 4, curves 3 and 4), the distribution of  $\text{Co}_{\text{Oh}}^{2+}$  ions at ion-exchange positions in the pore space of Co(*n*)ZSM-5 samples became more homogeneous, as evidenced by the appearance of a narrowed absorption band at  $17800\text{ cm}^{-1}$  in the diffuse reflectance electronic spectrum [12]. Moreover, the diffuse reflectance electronic spectrum of a Co(2.0)ZSM-5 sample (Fig. 4, curve 3) additionally exhibited a pair of absorption bands in the visible region at  $15300$  and  $16000\text{ cm}^{-1}$  due to the  $d$ – $d$  transition of  $\text{Co}_{\text{Td}}^{2+}$  cations, which are stabilized in HZSM-5 channels because of the interaction with extraframework  $\text{Al}^{3+}$  cations as one-dimensional  $\text{CoAl}_2\text{O}_4$  nanoanalog [12]. These one-dimensional  $\text{Co}^{2+}$  nanoaluminates were also formed at a 3.0 wt % cobalt content (Fig. 4, curve 4). It is likely that a shoulder at  $21000\text{ cm}^{-1}$ , which appeared in the diffuse reflectance electronic spectra of Co(2.0)ZSM-5 (Fig. 4, curve 3) and Co(3.0)ZSM-5 samples (Fig. 4, curve 4), was due to the  $d$ – $d$  transition of  $\text{Co}^{2+}$  ions in an octahedral coordination in the structure of one-dimensional clusters with the  $\text{CoO}$  stoichiometry. The absorption band at  $13000\text{ cm}^{-1}$  in the diffuse reflectance electronic spectrum of the Co(2.0)ZSM-5 sample (Fig. 4, curve 3) is difficult to interpret unambiguously because we were the first to observe its simultaneous appearance with the shoulder at  $21000\text{ cm}^{-1}$ .

Previously, the interaction of  $\text{Co}^{2+}$  and  $\text{Al}^{3+}$  salts with the formation of a  $\text{Co}^{2+}$  hydroxoaluminate (CHA) was observed in mixed aqueous solutions even at pH  $\sim 7.5$  [17]. Note that CHA with the constant cationic ratio  $\text{Co}/\text{Al} = 2 : 1$  was formed upon varying the  $\text{Co}/\text{Al}$  ratio in starting solutions from  $2.5 : 1$  to  $1 : 4$ . In the course of thermal treatment at  $T \geq 250^\circ\text{C}$ , the  $\text{CoAl}_2\text{O}_4$  spinel and  $\text{CoO}$  were formed from bulk CHA. According to our data, the  $\text{Co}^{2+}$  ions in the spinel exhibited mainly ( $\sim 85\%$ ) tetrahedral and partially ( $\sim 15\%$ ) octahedral coordinations or an octahedral oxygen coordination in the  $\text{CoO}$  oxide. It is believed that the interactions of  $\text{Co}^{2+}$  ions with extraframework  $\text{Al}^{3+}$  ions analogous to those described by Taraban et al. [17] occur in HZSM-5 channels after the incipient wetness impregnation of the zeolite with a solution of a  $\text{Co}^{2+}$  salt followed by an alkaline treatment. In this case, one-dimensional CHA nanoclusters are formed in zeolite micropores, whereas the formation of two- and three-dimensional CHA nanoparticles in mesopores would be expected. After thermal treatment at  $450^\circ\text{C}$ , the CHAs were converted into one- and three-dimensional nanoaluminates and  $\text{Co}^{2+}$  oxo compounds, respectively.

An absorption band multiplet at 15800, 17000, and 18300  $\text{cm}^{-1}$  (Fig. 4, curve 5), which corresponds to the diffuse reflectance electronic spectrum of bulk  $\text{CoAl}_2\text{O}_4$  [12], appeared in the diffuse reflectance electronic spectrum of zeolite  $\text{Co}(5.0)\text{ZSM-5}$ , which exhibited the maximum filling of mesopores with the modifying component among the entire sample series (see Table 1). It is likely that this multiplet masked absorption bands due to one-dimensional  $\text{Co}^{2+}$  nanoaluminates arranged in zeolite micropores in the diffuse reflectance electronic spectrum.

Thus,  $\text{Co}_{\text{OH}}^{2+}$  ions are stabilized in the following two forms in the pore space of modified  $\text{Co}(n)\text{ZSM-5}$  samples: at isolated ion-exchange positions and as one-dimensional  $\text{CoO}$  nanoclusters. Moreover, a very small fraction of  $\text{Co}_{\text{OH}}^{2+}$  can occur in three-dimensional  $\text{CoO}$  or  $\text{CoAl}_2\text{O}_4$  nanoparticles, the presence of which is evidenced by X-ray data given below. The  $\text{Co}_{\text{TD}}^{2+}$  cations in zeolite micropores are stabilized in the structure of one-dimensional  $\text{CoAl}_2\text{O}_4$  nanoclusters and, partially, as  $\text{CoAl}_2\text{O}_4$  nanocrystals in mesopores.

From an analysis of the entire set of diffuse reflectance electronic spectroscopy data, it follows that the stoichiometry of cobalt–oxygen fragments in the modifying component corresponds to  $\text{CoO}$  regardless of the nature and localization of this component in the zeolite pore space.

Figure 5 shows the diffraction patterns of the parent zeolite HZSM-5 and the samples with Co contents of 3.0 and 5.0 wt % in the range of angles  $2\theta = 5^\circ$ – $40^\circ$ . These data indicate that the cobalt-modified samples did not exhibit detectable shifts of peaks with respect to those of the parent zeolite. However, a redistribution of line intensities depending on Co content can be seen;

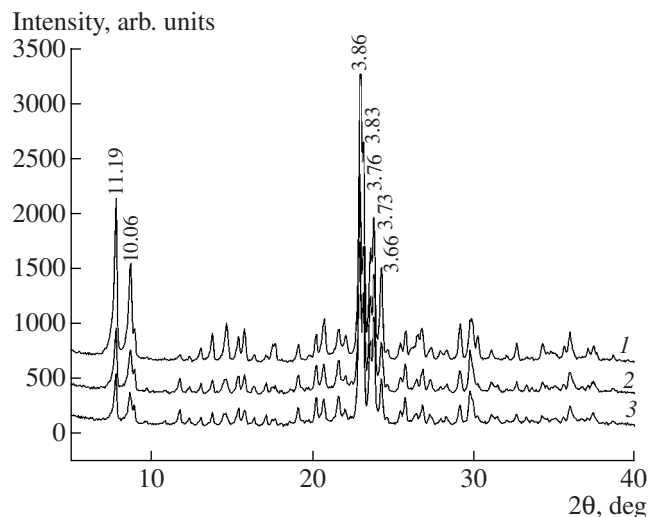
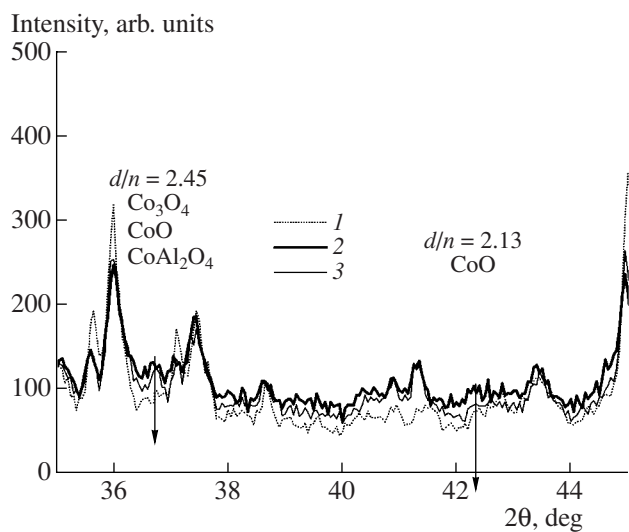


Fig. 5. Diffraction patterns of (1) parent zeolite HZSM-5 and  $\text{Co}(n)\text{ZSM-5}$  samples containing (2) 3.0 and (3) 5.0 wt % Co.

for example, the intensity of the strongest lines corresponding to the interplanar distances  $d/n = 11.19$ , 10.06, 3.86, 3.83, 3.76, 3.73, and 3.66 Å decreased with cobalt content. According to the above diffuse reflectance electronic spectroscopy data, the isomorphous replacement of  $\text{Al}_{\text{TD}}^{3+}$  by  $\text{Co}^{2+}$  cations was not observed. Thus, it is believed that the redistribution of line intensities in the diffraction patterns was due to the filling of the zeolite pore space with the modifying component; this is also consistent with sorption data. However, this process did not result in a detectable deformation of the zeolite framework.

Figure 6 shows the fragments of diffraction patterns in the range of angles  $2\theta = 35^\circ$ – $45^\circ$ , in which the most intense lines due to oxides and cobalt aluminate occurred:  $\text{Co}_3\text{O}_4$ ,  $d/n = 2.44$  Å (100%);  $\text{CoO}$ ,  $d/n = 2.46$  Å (67%) and  $d/n = 2.13$  Å (100%);  $\text{CoAl}_2\text{O}_4$ ,  $d/n = 2.44$  Å (100%). In Fig. 6, it can be seen that oxide phase impurities can occur in small amounts in the samples with cobalt contents of 3.0 and 5.0 wt %. A comparison between the adsorption and X-ray diffraction measurements and diffuse reflectance electronic spectroscopy data allowed us to conclude that the  $\text{Co}(3.0)\text{ZSM-5}$  and  $\text{Co}(5.0)\text{ZSM-5}$  samples contained three-dimensional  $\text{CoAl}_2\text{O}_4$  and  $\text{CoO}$  impurity nanocrystals arranged in zeolite mesopores with  $D < 5.0$  nm.

The experimentally found change in the pore volumes of samples as a result of modification allowed us to evaluate the effective density of the modifying component in the pore space of a matrix. In this case, it should be taken into account that, according to the diffuse reflectance electronic spectroscopy data, the stoichiometry of cobalt–oxygen fragments in modifying component nanoparticles is close to  $\text{CoO}$ . Correspondingly, the modifier weight should be increased, as com-



**Fig. 6.** Fragments of the diffraction patterns of (1) parent zeolite HZSM-5 and Co(n)ZSM-5 samples containing (2) 3.0 and (3) 5.0 wt % Co.

pared to the calculated value (given in sample designations), proportionally to a change in the molecular weight on going to the CoO stoichiometry:  $(59 + 16)/59 = 1.27$ .

Table 2 summarizes the estimations of the effective densities of the modifying component in the cobalt-containing samples ( $\rho_{\text{eff}} = m_{\text{CoO}}/\Delta V_s$ ) and the volume fractions of the modifying component in the micropore volume of zeolite HZSM-5 ( $\gamma = \Delta V_{\mu}/\Delta V_s$ ), where the parameter  $V_s$  corresponds to the limiting volume of the sorption space and  $\Delta V_s$  is the change in this parameter for modified samples, as compared with that of the parent zeolite. Correspondingly,  $\Delta V_{\mu}$  is the change in the zeolite micropore volume upon modification.

In Table 2, it can be seen that the nanodispersed modifying component in the zeolite pore space had a much lower (by a factor of 6) effective density than that of the bulk phase (e.g., 5.7–6.7 g/cm<sup>3</sup> for CoO [18]), and it was mainly arranged in the micropore volume (zeolite channels) as one-dimensional nanoclusters. The value of  $\gamma$  noticeably decreased with increasing concentration of the modifying component because of

**Table 2.** Texture parameters of the samples and the effective density of the nanodispersed cobalt-containing modifying component

Cobalt concentration in HZSM-5, %	$V_s$ , cm <sup>3</sup> /g	$\Delta V_s$ , cm <sup>3</sup> /g	$\rho_{\text{eff}}$ , g/cm <sup>3</sup>	$\gamma$
0	0.224	–	–	–
0.5	0.242	–	–	–
2.0	0.199	0.025	1.0	0.96
3.0	0.190	0.034	1.1	0.73
5.0	0.160	0.064	1.0	0.67

the arrangement of three-dimensional CoAl<sub>2</sub>O<sub>4</sub> and CoO nanocrystals in the mesoporous portion of the zeolite structure with pore sizes  $D < 5$  nm.

## ACKNOWLEDGMENTS

This work was supported by the Russian Foundation for Basic Research (project no. 06-03-33107).

## REFERENCES

1. Kazanskii, V.B., Serykh, A.I., and Bell, A.T., *Catal. Lett.*, 2002, vol. 83, nos. 3–4, p. 191.
2. Glebov, L.S., Zakirova, A.G., Tret'yakov, V.F., Burdeinaya, T.N., and Akopova, G.S., *Neftekhimiya*, 2002, vol. 42, no. 3, p. 163 [*Pet. Chem. (Engl. Transl.)*, vol. 42, no. 3, p. 143].
3. Shelef, M., *Chem. Rev.*, 1995, vol. 95, p. 209.
4. Armor, J.N., *Catal. Today*, 1995, vol. 26, p. 147.
5. Goryashchenko, S.S., Alimov, M.A., Fedorovskaya, E.A., Slovetskaya, K.I., and Slinkin, A.A., *Kinet. Katal.*, 1994, vol. 35, no. 4, p. 588.
6. Kucherov, A.V., Kucherova, T.N., Nissenbaum, V.D., and Slinkin, A.A., *Kinet. Katal.*, 1995, vol. 36, no. 5, p. 731.
7. Verberckmoes, A.A., Uytterhoeven, M.G., and Schoonheydt, R.A., *Zeolites*, 1997, vol. 19, no. 2/3, p. 180.
8. *Molecular Sieves*, vol. 3: *Science and Technology: Post-synthesis Modification I*, Karge, H.G. and Weitkamp, J., Eds., Berlin: Springer, 2002.
9. Rice, M.J., Chakraborty, A.K., and Bell, A.T., *J. Catal.*, 2000, vol. 194, no. 2, p. 278.
10. Dedecek, J., Kaucky, D., Wichterlova, B., and Gonsiorova, O., *Phys. Chem. Chem. Phys.*, 2002, vol. 4, no. 21, p. 5406.
11. Paukshtis, E.A., *Infrakrasnaya spektroskopiya v geterogennom kislotno-osnovnom katalize* (Infrared Spectroscopy in Heterogeneous Acid–Base Catalysis), Novosibirsk: Nauka, 1992.
12. Krivoruchko, O.P., Anufrienko, V.F., Paukshtis, E.A., Larina, T.V., Burgina, E.B., Yashnik, S.A., Ismagilov, Z.R., and Parmon, V.N., *Dokl. Akad. Nauk*, 2004, vol. 398, no. 3, p. 356 [*Dokl. Phys. Chem. (Engl. Transl.)*, vol. 398, no. 3, p. 226].
13. Karnaukhov, A.P., *Adsorbsiya: Tekstura dispersnykh i poristykh materialov* (Adsorption: Texture of Disperse and Porous Materials), Novosibirsk: Nauka, 1999.
14. Gregg, S.J. and Sing, K.S.W., *Adsorption, Surface Area and Porosity*, London: Academic, 1982.
15. Lever, A.B.P., *Inorganic Electronic Spectroscopy*, Amsterdam: Elsevier, 1987.
16. Mott, N. and Davis, E., *Electronic Processes in Non-Crystalline Materials*, Oxford: Oxford Univ., 1979.
17. Taraban, E.A., Malakhov, V.V., Krivoruchko, O.P., Plyasova, L.M., and Boldyreva, N.N., *Zh. Neorg. Khim.*, 1991, vol. 36, no. 4, p. 875.
18. Rabinovich, V.A. and Khavin, Z.Ya., *Kratkii khimicheskii spravochnik* (Concise Handbook of Chemistry), Potekhin, A.A. and Efimov, A.I., Eds., St. Petersburg: Khimiya, 1994.